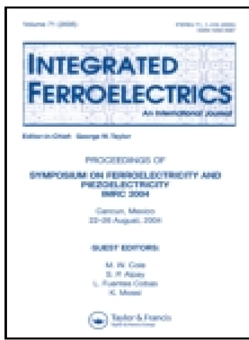

Taylor & Francis
Taylor & Francis Group

Integrated Ferroelectrics

ISSN: 1058-4587 (Print) 1607-8489 (Online) Journal homepage: http://www.tandfonline.com/loi/ginf20

Texturing and electrical characteristics of sol-gel derived ferroelectric thin films

Kwangsoo No , Chang Jung Kim , Dae Sung Yoon , Joon Sung Lee , Chaun Gi Choi , Won Jong Lee & Byeong Soo Bae

To cite this article: Kwangsoo No , Chang Jung Kim , Dae Sung Yoon , Joon Sung Lee , Chaun Gi Choi , Won Jong Lee & Byeong Soo Bae (1995) Texturing and electrical characteristics of sol-gel derived ferroelectric thin films, Integrated Ferroelectrics, 9:1-3, 159-168, DOI: 10.1080/10584589508012920

To link to this article: https://doi.org/10.1080/10584589508012920

Published online: 19 Aug 2006.

Submit your article to this journal

Article views: 10

Citing articles: 1 View citing articles

Full Terms & Conditions of access and use can be found at
http://www.tandfonline.com/action/journalInformation?journalCode=ginf20

Integrated Ferroelectrics, 1995, Vol. 9, pp. 159-168
Reprints available directly from the publisher
Photocopying permitted by license only

© 1995 OPA (Overseas Publishers Association)
Amsterdam B.V. Published under license by
Gordon and Breach Science Publishers SA
Printed in Malaysia

TEXTURING AND ELECTRICAL CHARACTERISTICS OF SOL-GEL DERIVED FERROELECTRIC THIN FILMS

KWANGSOO NO, CHANG JUNG KIM, DAE SUNG YOON, JOON SUNG LEE, CHAUN GI CHOI, WON JONG LEE*, BYEONG SOO BAE

Dept. of Ceramic Science and Engineering, *Dept. of Electronic Materials Science and Engineering, Korea Advanced Institute of Science and Technology, Yusong Gu, Kusung dong 373-1, Taejon, Korea

(Received November 21, 1994)

Abstract Highly oriented PZT, PLZT and PMN thin films were fabricated on various substrates using sol-gel method. The thin films having different orientation were fabricated by different drying conditions for pyrolysis. The preferred orientations of the PZT, PLZT and PMN thin films were observed using XRD(X-ray diffraction). The hysteresis loops, capacitance-voltage, and fatigue characteristics of the films were investigated using an RT66A standardized ferroelectric test system. The dielectric constant and current-voltage characteristics of the films were investigated using impedance analyzer and pA meter, respectively. The films oriented in particular direction showed better electrical characteristics to the randomly oriented films.

INTRODUCTION

Recently, various deposition methods have been carried out for PZT and PLZT thin films because of their potential applications in piezoelectric and pyroelectric devices and non-volatile memories.[1-3] However, ferroelectric fatigue and leakage current have been major obstacles in the practical applications of the films for electronic devices. In order to improve the electrical properties, the thin film has been fabricated in such a way as to grow epitaxially or preferentially. For texturing of sol-gel derived thin films, it is necessary to use single crystal substrates[4] and to control processing variables such as type of solvent, catalyst and drying temperature[5].

In this paper, we present methods of preparing highly oriented PZT, PLZT and PMN films on various substrates using the sol-gel method. Dielectric constant, P-E hysteresis loops, capacitance-voltage characteristics and current-voltage characteristics of highly oriented PZT and PLT films will be reported.

EXPERIMENTAL PROCEDURE

The PZT composition and the substrate used in this study were 52/48 and Pt/Ti/Corning 7059 glass, respectively. The PLZT precursor solution was prepared using lead acetate ($Pb(CH_3COO)_2 \cdot 3H_2O$), zirconium n-propoxide ($Zr(C_3H_7O)_4$) and titanium i-propoxide ($Ti[(CH_3)_2CHO]_4$). The PMN precursor solution was prepared using lead acetate, magnesium ethoxide($Mg(C_2H_5O)_2$) and niobium ethoxide($Nb(C_2H_5O)_5$). 2-methoxyethanol($CH_3CH_2CH_2OH$) was used as solvent. The detailed report of the solution preparation method was described in Ref. 5. The solution was spin coated at 3000 rpm for 30 seconds onto substrate. The coated film was dried at the temperature range of 270 ℃ to 350 ℃ for 5 min for pyrolysis. This coating and drying procedure was repeated 9 times to obtain desired thickness of around 0.5μm. Single crystal substrates ($SrTiO_3$, MgO, sapphire and Pt/MgO) were used to obtain epitaxial PLZT thin films. Glass substrate with a PLT layer with a thickness of about 50 nm was used to obtain textured PLZT thin films which contain higher Zr content. The thin layer serves as a seeding layer to accelerate the formation of the oriented nuclei. We also controlled the processing variables such as the type of solvent and the drying temperature to change the crystal orientation of the PMN and the PZT thin films, respectively. The coated P(L)ZT films were then reacted for crystallization at 600 ℃ and 650 ℃ using the direct insertion[6] and RTP for 20 min and 1 min, respectively. The PMN films were reacted at 750 ℃ using the direct insertion method for 20 min. The crystallinity and the grain orientation of the films were observed using XRD. The P-E hysteresis, the capacitance-voltage, and the fatigue characteristics of the films were evaluated using an RT66A standardized ferroelectric test system. The dielectric constant and current density-voltage characteristics of the films were measured using an impedance analyzer and a pA meter, respectively.

RESULTS AND DISCUSSION

Texturing of Sol-gel Derived Thin Films.

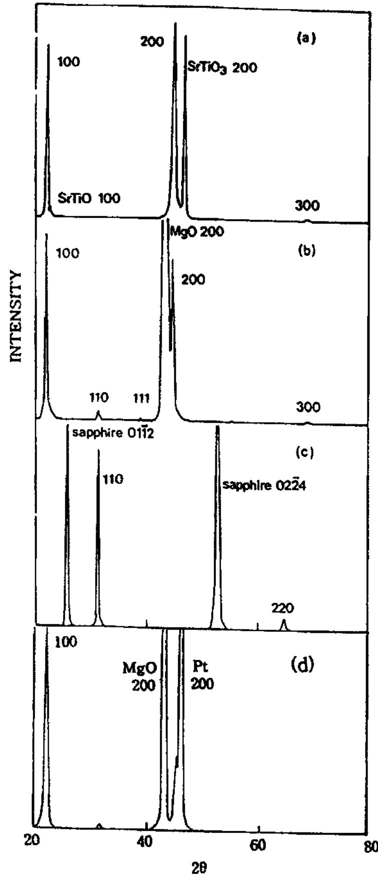

Fig. 1. XRD patterns of the PLZT(9/50/50) on (a) $SrTiO_3$(100), (b) MgO(100) and (c) r-plane sapphire, and the PLT(10/0/100) film on (d) Pt/Ti/MgO.

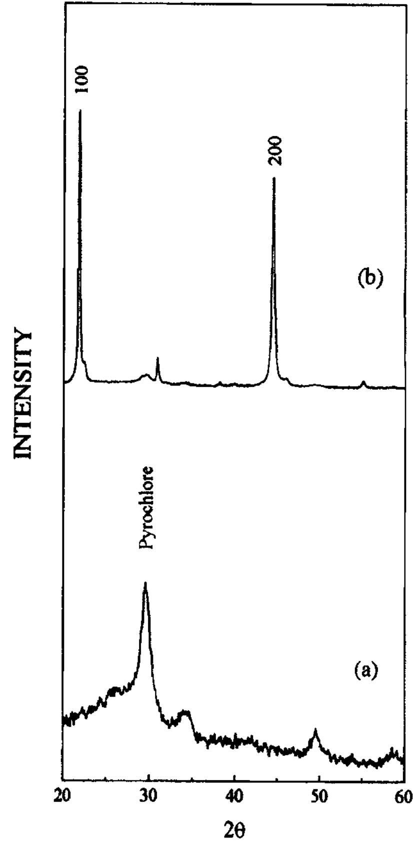

Fig. 2. XRD patterns of the PLZT thin films (a) without and (b) with a seeding layer on glass substrates

In the sol-gel processing, single crystal substrate is one of the most convenient methods to obtain textured ferroelectric thin films. We used $SrTiO_3$, MgO, sapphire and Pt/Ti/MgO substrates. X-ray Diffraction patterns of the PLZT thin films fabricated on the single crystal substrates are shown in Figure 1. From the XRD patterns, it is known that the PLZT(100) for the $SrTiO_3$, the PLZT(110) for the sapphire, and the PLT(100) for the Pt/Ti/MgO are parallel to the surface of the substrates. The XRD patterns of the films on an MgO

show minor extra peaks of (110) and (111) with main (100) and (200) peaks, indicating that the PLZT films on the substrate were grown with preferred orientation.

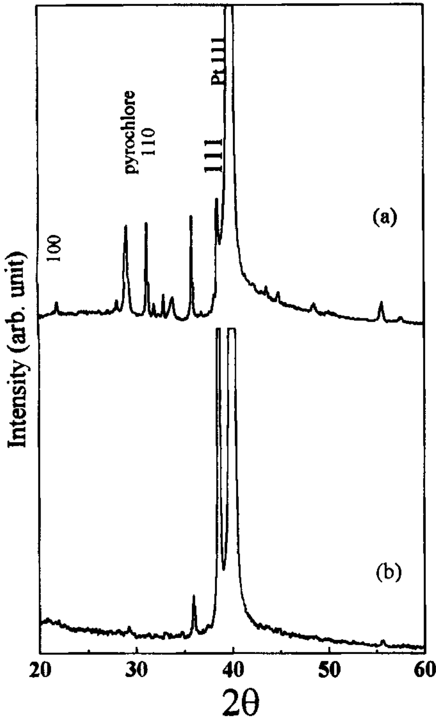

Fig. 3. XRD patterns of the PMN films made of the solutions with the solvents of (a) 100 % methoxy-ethanol and (b) 50 % propanol + 50 % methoxyethanol.

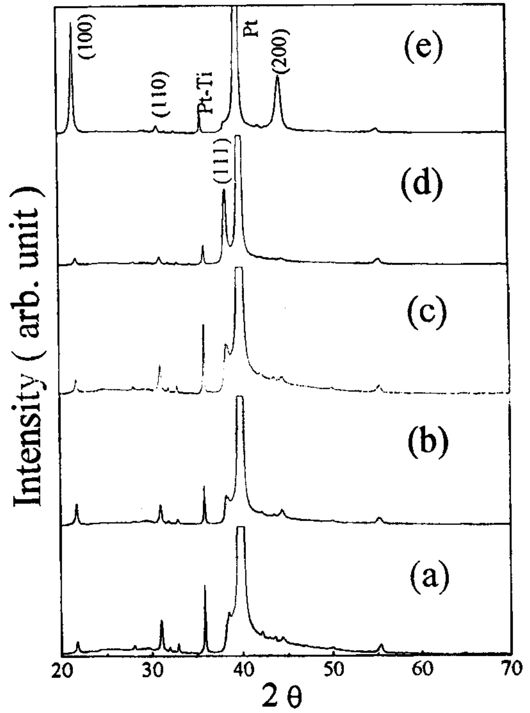

Fig. 4. XRD patterns of the PZT(52/48) dried at (a) 270 ℃, (b) 290 ℃, (c) 310 ℃, (d) 330 ℃ and (e) 350 ℃.

Amorphous substrates are not suitable for the textured growth of the sol-gel films, because they have random atom arrangement. Coated on an amorphous substrate, the thin PLT layer (50 nm) consists of (100) aligned perovskite grains. Therefore, the thin layer may serve as a seeding layer to accelerate the formation of oriented nuclei in the film. Figure 2 shows the XRD patterns of the PLZT(9/65/35) thin films with and without the PLT seeding layers heat-treated at the same temperature(600 ℃). The XRD pattern of the PLZT(9/65/35) thin film without the seeding layer consists of pyrochlore and amorphous phase peaks. It was confirmed that the glass is not a good

substrate for the formation of the perovskite phase for the PLZT(9/65/35) thin film. The XRD pattern of the PLZT(9/65/35) film with seeding layer consists of strong (100) and (200) perovskite peaks, indicating that the film grew with the preferred (100) orientation.

Changing the solvent of the PMN coating solution, we could fabricate the highly (111) oriented PMN thin films. Figure 3(a) and (b) show the XRD patterns of the PMN thin films made of the coating solutions with solvents of 100 % methoxyethanol and 50 % methoxyethanol + 50 % propanol, respectively. The PMN thin film made with 100 % methoxyethanol consists of the polycrystalline pyrochlore phase and has no preferred orientation. However, the PMN thin film made with 50 % methoxyethanol + 50 % propanol consists of the full perovskite phase and shows the (111) preferred orientation. When the amorphous PMN film was fired at higher temperature(850 ℃), Pb loss led to the nonstoichiometric composition of the film and resulted in the formation of the pyrochlore phase.

Dried at different temperatures, the sol-gel thin film consisted of different contents of organic residue observed in the FT-IR spectra[7]. It was found that the organic residue in the film affected the crystallization behavior of the sol-gel thin film at the final reaction. The PZT films coatedon Pt/Ti/glass were dried at different temperatures for pyrolysis and then finally reacted at the same temperature of 650 ℃ using RTA for 1 min. Figure 4 shows the XRD patterns of the PZT thin films dried at different temperatures. All films completely consist of the perovskite PZT phase without the pyrochlore phase. The films heat treated for pyrolysis at and below 310 ℃ consist of the perovskite phase with a random orientation. However, The films heat treated at 330 ℃ and 350 ℃ [Fig. 4(d) and (e)] show strong (111) and (100) preferred orientation, respectively.

Electrical Properties of Epitaxial PLT(10/0/100) Films on Pt/Ti/MgO.

Electrical properties of the epitaxial and the polycrystalline PLT thin films were measured. We prepared the epitaxial and the polycrystalline PLT film on Pt(100)/Ti/MgO and Pt(111)/Ti/MgO, respectively. Figure 5 shows dielectric constant-frequency characteristics of both PLT thin films. Both PLT thin films showed slow decrease throughout all frequencies measured in this study. The epitaxial PLT thin film has a dielectric constant of about 738 at 1kHz. The

dielectric constant of the polycrystalline films is about 540 at 1kHz. The dielectric constant of the epitaxial film is about 200 higher than that of the polycrystalline film in low frequency region.

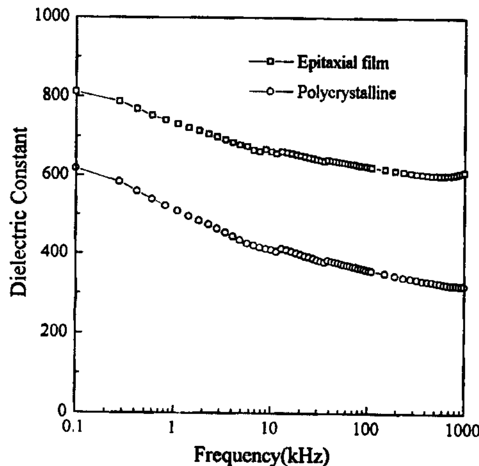

Fig. 5. Dielectric constant vs. frequency characteristics of the epitaxial and the polycrystalline PLT films.

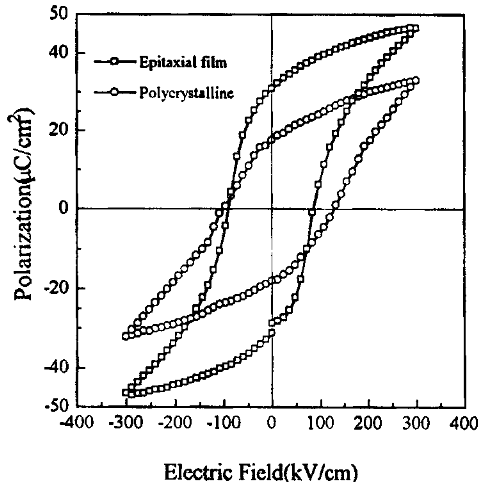

Fig. 6. Hysteresis loops of the epitaxial and the polycrystalline PLT films.

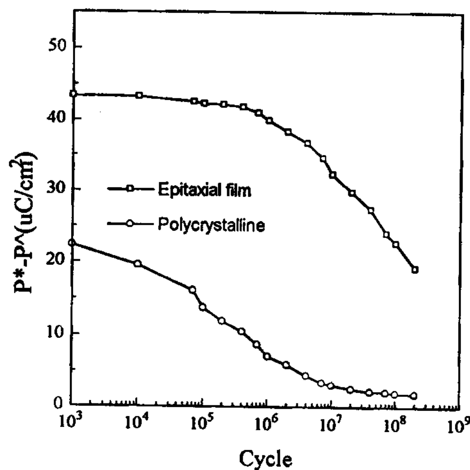

Fig. 7. Fatigue characteristics of the epitaxial and the polycrystalline PLT film.

The ferroelectricity of the epitaxial and the polycrystalline PLZT(10/0/100) thin films were investigated by observing the polarization hysteresis using RT66A ferroelectric testing system. Figure 6 shows a family of hysteresis loops measured with applying maximum voltage of ±15 V. The spontaneous

polarization(Ps) and the remanent polarization(Pr) of the epitaxial thin film are 51.2 μC/cm^2 and 35.5 μC/cm^2, respectively. The coercive field(Ec) of the film is 91.8 kV/cm. The hysteresis loop of the polycrystalline film shows a spontaneous polarization of 33.2 μC/cm^2, a remanent polarization of 18.2 μC/cm^2 and a coercive field of 124.2 kV/cm. The epitaxial thin films has better squareness and much higher polarization values(Ps and Pr) than the polycrystalline thin film.

We used the pulsed polarization method to measure the fatigue of the PLZT thin films. Because the switching polarization(P*) and non-switching polarization(P^) are important in the memory operation, the fatigue effects were analyzed in terms of these polarizations. Figure 7 shows the fatigue curves of the two films measured under the maximum applied voltage of ±10 V. Bipolar cycling decreases the difference between the switching polarization(P*) and the non-switching polarization(P^) rapidly after 10^6 cycles in the case of the epitaxial film. The difference of the polycrystalline film decreases readily throughout all cycles. The value of (P* - P^) after 10^8 cycling is about 18.5 μC/cm^2 for the epitaxial film whereas it is about 2.1 μC/cm^2 for the polycrystalline film. From above results, it may be speculated that the epitaxial PLZT thin films have better fatigue characteristics than the polycrystalline films.

Electrical Properties of Highly Oriented PZT Films on Pt/Ti/Glass.

Figure 8 shows the polarization versus electric field hysteresis loops of the (100), the (111) and the randomly oriented films. The spontaneous polarization(Ps), the remnant polarization(Pr), and the coercive field(Ec) of the randomly oriented film are 33.7 μC/cm^2, 5.1 μC/cm^2, and 40.3 kV/cm, respectively. The Ps, the Pr and the Ec of the (111) aligned film are 48.9 μC/cm^2, 17.4 μC/cm^2, and 83.7 kV/cm, respectively. The Ps, the Pr and the Ec of the (100) aligned film are 38.1 μC/cm^2, 10.4 μC/cm^2, and 58.8 kV/cm, respectively. The (111) aligned film has much higher polarization values (Ps and Pr) and Ec than the (100) and the randomly aligned films, which indicates that the domain switching is harder in the (111) aligned film than in the (100) and the randomly aligned films. An asymmetric hysteresis loop was observed for the (111) aligned film and a nearly symmetric hysteresis loop was observed for the (100) aligned film, which were also observed in the other study[8].

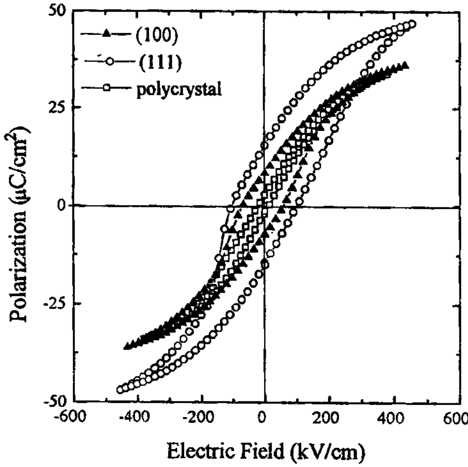

Fig. 8. Hysteresis loops of the (100), the (111) and the randomly oriented PZT films.

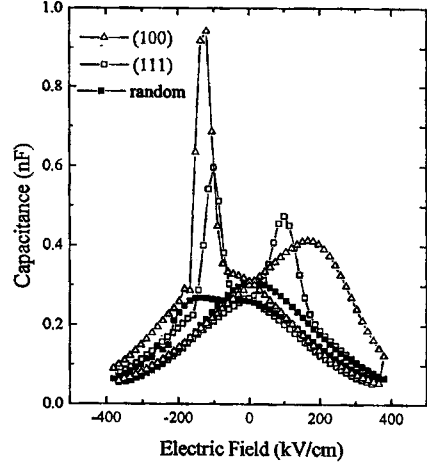

Fig. 9. Capacitance vs. voltage characteristics of the (100), the (111) and the randomly oriented PZT films.

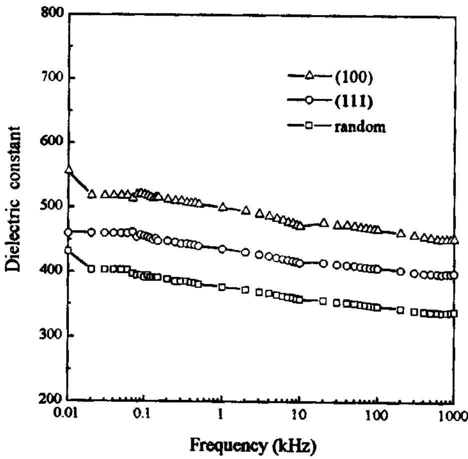

Fig. 10. Dielectric constant-frequency characteristics of the (100), the (111) and the randomly oriented PZT films.

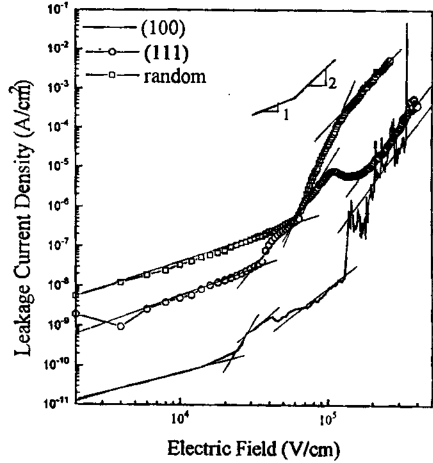

Fig. 11. Current density-electric field characteristics of the (100), the (111) and the randomly oriented PZT films.

Figure 9 shows the capacitance-voltage (C-V) characteristics of the (100), the (111) and the randomly oriented films. For the randomly oriented film, the C-V curve was shifted in the direction of negative bias. The reason for such a shift may lie in either the fixed charge which forms due to the nonswitching part of spontaneous polarization or other structural defects in the ferroelectric films.[9] But, the thin films aligned in particular directions show the coincidence

of the maximum voltage between the negative and the positive bias. Asymmetric C-V curves were observed for the (100) and the (111) aligned films. The (111) aligned film showed a larger asymmetric curve than the (100) aligned film. These asymmetric C-V curves may be due to the induced asymmetric space charge that was derived by the self-aligned spontaneous polarization in the films.

Figure 10 shows the dielectric constant-frequency characteristics of the (100), the (111) and the randomly oriented films. The (100), the (111), and the randomly oriented films have dielectric constants of about 549, 453, and 376 at 1 kHz, respectively. The dielectric constants of the (100) aligned film are higher than those of both the (111) aligned and the randomly oriented films in the measured frequency range. Abrupt dielectric constant change in the low frequency region may be due to the space charge polarization formed between the electrode and the thin film.

Figure 11 shows the current density-voltage characteristics of the (100), the (111) and the randomly oriented films. All films showed three regions having different slopes. There are several types of the leakage current mechanisms in PZT thin films.[10] The leakage current densities at the electric field of 36 kV/cm were 1.31×10^{-9} A/cm^2 for the (100) aligned film, 4.12×10^{-8} A/cm^2 for the (111) aligned film and 1.84×10^{-7} A/cm^2 for the randomly oriented film. The thin films aligned in particular directions show lower leakage current density in the ohmic region than the randomly oriented film.

SUMMARY

We prepared the epitaxial and the highly oriented P(L)ZT and PMN thin films on various substrates using sol-gel method. The epitaxial PLT thin film had higher dielectric constant and better ferroelectricity and fatigue resistance than the polycrystalline film. The (100) and (111)-oriented PZT films on Pt/Ti/glass had higher dielectric constant and better ferroelectricity and leakage current characteristics than the randomly oriented film.

REFERENCE

1. T. Tamagawa, D. L. Polla, and C.-C. Hseuch, IEEE International Elecrtron Device Meeting, San Francisco, Dec. 1990, p. 617.
2. D. L. Polla, Chian-Ping Ye and Takashi Tamagawa, Appl. Phys. Lett. 59(27), 3539 (1991).
3. C. A. Araujo, L. D. McMillan, B. M. Melnick, J. D. Cuchiaro, and J. F. Scott, Ferroelectrics, **104**, 241 (1990).
4. D. S. Yoon, C. J. Kim, W. J. Lee and K. No, J. Mater. Res., 9(2), 420 (1994).
5. C. J. Kim, D. S. Yoon, J. S. Lee, W. J. Lee and K. No, J. Appl. Phys., (in press).
6. D. S. Yoon, J. M. Kim, K. C. Ahn and K. No, Integrated Ferroelectrics, **4**, 93 (1994).
7. C. J. Kim, D. S. Yoon, J. S. Lee, C. G. Choi, W. J. Lee and K. No, J. Mater. Res., (in press).
8. R. Takayama and Y. Tomita, J. Appl. Phys., 65(4), 1666 (1989).
9. K. A. Vorotilov, M. I. Yanovskaya and O. A. Dorokuova, Integrated Ferroelectrics, **3**, 33 (1994).
10. H. Y. Lee, K. C. Lee, J. N. Schunke and L. C. Burton, IEEE Transaction on Components, Hybrids and Manufacturing Technology, **7**, 443 (1984).